Biogeosciences Discuss., 8, 2259–2280, 2011
www.biogeosciences-discuss.net/8/2259/2011/
doi:10.5194/bgd-8-2259-2011

Biogeosciences Discussions

Sedimentary organic matter variations in the Chukchi Borderland over the last 155 kyr

S. F. Rella and M. Uchida

National Institute for Environmental Studies, Environmental Chemistry Division, Onogawa 16–2, Tsukuba 305–8506, Japan

Received: 15 February 2011 – Accepted: 18 February 2011 – Published: 4 March 2011

Correspondence to: S. F. Rella (stephanrella@gmail.com)

Published by Copernicus Publications on behalf of the European Geosciences Union.

Abstract

Knowledge on past variability of sedimentary organic carbon in the Arctic Ocean is important to assess natural carbon cycling and transport processes related to global climate changes. However, the late Pleistocene oceanographic history of the Arctic is still poorly understood. In the present study we show sedimentary records of total organic carbon (TOC), C/N and $CaCO_3$ from a piston core recovered from the northern Northwind Ridge in the far western Arctic Ocean, a region potentially sensitively responding to past variability in surface current regimes and sedimentary processes such as coastal erosion. An age model based on correlation of our $CaCO_3$ record with the benthic $\delta^{18}O$ stack, supplemented by lithological constraints, suggests that the piston core records paleoenvironmental changes of the last 155 kyr. According to this age model, TOC and C/N show orbital-scale increases and decreases that can be respectively correlated to the waxing and waning of large ice sheets dominating the Eurasian Arctic, suggesting advection of fine suspended matter derived from glacial erosion to the Northwind Ridge by eastward flowing intermediate water and/or surface water and sea ice during cold episodes of the last two glacial-interglacial cycles. At millennial scales, increases in TOC and C/N appear to correlate to a suite of Dansgaard-Oeschger Stadials between 120 and 40 ka before present (BP) and thus seem to respond to abrupt northern hemispheric temperature changes. Between 65 and 40 ka BP, closures and openings of the Bering Strait could have additionally influenced TOC and C/N variability. $CaCO_3$ content tends to anti-correlate with TOC and C/N on both orbital and millennial time scales, which we interpret as enhanced sediment advection from the carbonate-rich Canadian Arctic via an extended Beaufort Gyre during warm periods of the last two glacial-interglacial cycles and increased terrestrial organic carbon advection from the Siberian Arctic during cold periods when the Beaufort Gyre contracted. We propose that this pattern may be related to orbital- and millennial-scale variations of dominant atmospheric surface pressure systems expressed in mode shifts of the Arctic Oscillation.

BGD

8, 2259–2280, 2011

Sedimentary organic matter variations in the Chukchi Borderland

S. F. Rella and M. Uchida

1 Introduction

The causes and implications of recent climate change are intensively debated. In particular the Arctic region appears to respond sensitively to climate change, as demonstrated by a continuous decrease in sea ice extent over the last 30 yr (Johannessen et al., 2004). Arctic environmental change directly relates to changes in total organic carbon (TOC) in Arctic Ocean sediments through variable terrestrial and marine input of organic matter. Today, coastal erosion and to a lesser extent large rivers such as the Yenisei and Lena play the dominant role for terrestrial organic carbon (OC_{terr}) input along the coasts of Siberia and Alaska (Reimnitz et al., 1988; Rachold et al., 2000). In the Canadian Beaufort Sea, on the other hand, river discharge from the Mackenzie River is more important than coastal erosion (Macdonald et al., 1998). Marine organic carbon (OC_{mar}) accumulation is mainly limited by the extents of sea ice, which decreases surface productivity by one order of magnitude compared to open water conditions (Wollenburg and Mackensen, 1998). Thus, past variations in TOC deposition in Arctic Sea sediments provide a sensitive tool for tracking environmental changes that can be related to processes at land and sea, such as glacial erosion by ice sheets, river discharge, ocean circulation patterns and marine productivity. However, the orbital- to millennial-scale TOC variations in the far western and far eastern Arctic are poorly known, despite their importance for our understanding of sedimentary processes in relation to environmental change, for example through openings and closures of the Bering Strait (Hu et al., 2010). Here we present records of TOC, calcium carbonate ($CaCO_3$) and the ratio of TOC to total nitrogen (C/N) over the last 155 000 yr (155 kyr) from a sediment core recovered from the northern Northwind ridge, an area potentially strongly responding to climate change through changing ocean currents such as the Beaufort Gyre, summer sea ice extent, as well as variable marine and terrigenous organic matter supply.

BGD
8, 2259–2280, 2011

2 Present and past oceanographic setting

The Chukchi Borderland, located about 1000 km north of the Bering Strait, is characterized by a complex topography of ridges and plateaus, which extend northward from the Chukchi Shelf into the Amerasian Basin (Fig. 1). Today, the area is primarily influenced by Pacific waters entering through the Bering Strait and a clockwise current in the Canada Basin known as Beaufort Gyre (e.g. Macdonald et al., 2003). The Beaufort Gyre transports sea ice and sediments from the Canadian Arctic to the Central Arctic (Stein, 2008). As a result of nutrient-rich Pacific water influx and open waters in summers, the contribution of OC_{mar} in the surface sediments of the Chukchi Borderland is relatively high (50% of TOC) (Naidu et al., 2004; Belicka and Harvey, 2009), compared to common average values of 10 to 20% in the Arctic Ocean due to significant input of OC_{terr} from the surrounding continents (Stein, 2008). At depths between ~200 and ~800 m, the Chukchi Borderland is influenced by the so called Atlantic Layer, an intermediate water mass inflowing from the Atlantic into the Arctic Ocean along the slopes of the Eurasian shelves (Fig. 1). Beneath the Atlantic Layer deep bottom water fills the Amerasian and Eurasian Basin.

The adjacent Chukchi Shelf encompasses an area of 620×10^3 km^2 with a mean depth of ~80 m. Due to its shallow depth the Chukchi Shelf was largely exposed during the Last Glacial Maximum (LGM) ca. 22 000 to 19 000 yr before present (22 to 19 ka BP), when sea level was ~120 m lower than today. During Marine Isotope Stage (MIS) 2, 6, and partly MIS 3 and 4 the Bering Strait was closed (Hu et al., 2010) owing to its shallow depth of only ~50 m today, inhibiting the inflow of Pacific waters.

During glacial periods large ice sheets dominated the shelves and adjacent land of western Siberia, the Canadian Arctic and Greenland (Dowdeswell et al., 2002). These ice sheets played an important role in transporting sediments to the shelf break through glacial erosion, sediment mass wasting (Dowdeswell et al., 1998, 2002) and calving of icebergs (e.g. Josenhans et al., 1986; Shipp et al., 2002). A fraction of the sediments is further transported from the shelf break of the Barents and Kara seas far to the east

BGD
8, 2259–2280, 2011

via the Atlantic Layer (Knies et al., 2001). Sea ice drifting transports sediments along prevailing surface currents, which depend on dominant wind patterns (e.g. Bischof and Darby, 1997). Iceberg scour marks on deeper parts of the Chukchi Shelf and on the Chukchi Borderland at depths shallower than 1000 m suggest movement of icebergs, possibly during the LGM and early deglaciation (Josenhans et al., 1986; Shipp et al., 2002).

3 Methodology

3.1 Core location and description

Piston core MR08-04 PC1 has been recovered in summer 2008 at 998 m water depth from the northern part of the Northwind Ridge (74°48.50′ N, 158°31.85′ W) (Fig. 1). Based on visual core inspection and soft X-ray radiographs, taken using a SOFTEX PRO-TEST 150, the core mainly consists of grey to olive brown clayey sediments (Fig. 2). A light brown interval can be observed between 520 and 572 cm below seafloor (cmbsf) and a pink-white layer between 539 and 543 cmbsf. Millimeter-scale laminations occur between 17 and 51, 630 and 637, and 679 and 690 cmbsf. PC1 is also characterized by several layers of mm-scale scattered IRD and isolated cm-scale IRD clasts (Fig. 2).

3.2 Carbon and nitrogen measurements

For the measurement of bulk carbon (C) and nitrogen contents, 1 to 1.5 g of freeze-dried sediments per sample were powdered, wrapped in tin capsules and measured using a CHN analyzer (EA1112, EURO SCIENCE) at the National Institute for Environmental Studies in Tsukuba. For TOC measurements, 1 g sediment per sample was treated with 1N HCL overnight to dissolve $CaCO_3$, washed three times using distilled water and dried in an oven overnight at 50 °C prior to powdering and measurement

BGD
8, 2259–2280, 2011

Title Page
Abstract Introduction
Conclusions References
Tables Figures
◂◂ ▸▸
◂ ▸
Back Close
Full Screen / Esc
Printer-friendly Version
Interactive Discussion

by CHN. At a few distinct horizons in the lower part of the core, TOC shows several relatively high single peaks with values between 1 and 7%, which need repeated measurement for validation and are therefore not included in this study. The percentage of $CaCO_3$ in the sediments has been approximated using the equation

$$\%CaCO_3 = (\%C - \%TOC) \times (100/12) \quad (1)$$

where the factor 100/12 corresponds to the atomic weight ratio of C and TOC. We also employ the C/N ratio in this study, which can be used as a measure of the relative contribution of OC_{terr} and OC_{mar}. C/N of OC_{mar} is around 6, while OC_{terr} is characterized by C/N values larger than 15 (Bordowskiy, 1965a, b). C/N is usually assumed to dominantly represent the ratio of TOC and organic nitrogen, because inorganic nitrogen (N_{inorg}) is comparatively low. However, when TOC is lower than ~0.5%, N_{inorg} may contribute more importantly to the variation of total nitrogen (Stein, 2008).

4 Results

4.1 Age model

Because radiocarbon dating of planktonic foraminifera has not yet been conducted, we relied on (a) down-core variations of $CaCO_3$ that show high similarity to the LR04 benthic $\delta^{18}O$ stack (Lisiecki and Raymo, 2005) and (b) colour and lithology changes of the sediments.

4.1.1 Age constraints based on variations in $CaCO_3$

Variation of $CaCO_3$ with depth is presented in Fig. 3. $CaCO_3$ in PC1 is low between core bottom and 676 cmbsf, and between 65 cmbsf and core top with values ranging from ~0.2 to ~5%. Between 902 and 461 cmbsf, $CaCO_3$ is high ranging from 17 to 28% and averaging ~22%, except for a negative excursion at ~504 cmbsf, where values decrease to 6.1%. Between 461 and 70 cmbsf, $CaCO_3$ averages ∼11% cyclically showing relatively increased values (∼8 to ∼17%) between 420 and 374, 330 and 292, 212 and 151, and 125 and 76 cmbsf. Between these layers of increased values, $CaCO_3$ is relatively low ranging from ∼5 to ∼10%.

Ice-rafted debris (IRD) on the Northwind Ridge is characterized by relatively high detrital carbonate contents, which are associated with sediment transport from the carbonate-rich Canadian Arctic via the Beaufort Gyre (Phillips and Grantz, 2001). Spielhagen et al. (1997, 2004) found increases in detrital $CaCO_3$ at the southeastern Lomonosov Ridge during MIS 7 and middle MIS 5, which could be explained by substantial sediment transport via an extended Beaufort Gyre during interglacial periods (Phillips and Grantz, 2001). Evidence for advection of detritus from the Canadian Arctic at site PC1 comes from the occurrence of a pink-white layer between 543 and 547 cmbsf in association with high $CaCO_3$ (Fig. 3). Furthermore, warm intervals of the last glacial-interglacial cycle would have promoted marine productivity and biogenic $CaCO_3$ deposition due to prolonged periods of open waters. We accordingly expect relative increases in total CaCO3 at site PC1 to mainly correspond to warm periods.

As illustrated in Fig. 3, the LR04 benthic $\delta^{18}O$ stack and $CaCO_3$ show distinct similarities in their respective variations. Periods of relatively light and heavy $\delta^{18}O$ in LR04, which are primarily related to decreased and increased global ice volume, respectively, could be correlated to similar periods of increased and decreased $CaCO_3$, both in amplitude and period length. Thus, following our suggestion of increased detrital and biogenic $CaCO_3$ at site PC1 during warm episodes, we construct a preliminary age model for PC1 by correlating five distinct horizons of low $CaCO_3$ to increased $\delta^{18}O$ in LR04 (Fig. 3). According to this age model, the sedimentation rate of the core is relatively constant at ∼5 cm kyr^{-1}, which is a reasonable value for cores recovered from ridges such as the Northwind Ridge in the Arctic Ocean for the last glacial-interglacial cycle (e.g. Backman et al., 2004).

BGD
8, 2259–2280, 2011

Sedimentary organic matter variations in the Chukchi Borderland

S. F. Rella and M. Uchida

4.1.2 Age constraints based on colour and lithology

Arctic Ocean sediments deposited during interglacial periods are typically of brown colour (e.g. Phillips and Grantz, 1997), and characterized by strong bioturbation, while glacial deposits are typically of greyish colour, and characterized by a low degree of bioturbation or laminations (absence of bioturbation) (Stein, 2008). According to our carbonate-based age model, the light brown layer between 520 and 572 cmbsf correlates very well with the $CaCO_3$ maximum during MIS 5e, while the laminations correlate to the glacial maxima of MIS 6 and MIS 2 (Fig. 3). Laminations during glacial maxima can be expected in the western Arctic, as the LGM was probably characterized by perennial sea ice cover (Darby et al., 1997) and strongly limited benthic fauna (Wollenburg and Mackensen, 1998). Changes in lithology and colour in PC1 therefore support our carbonate-based age model.

4.2 Temporal variations of TOC and C/N during the last 155 kyr at site PC1

The temporal variation of TOC at site PC1 is shown in Fig. 4. TOC values range between ~0.15 and ~0.45% during the last 155 kyr, punctuated by major peaks at 135, 130, 125, 117, 65, 59, 55, 47, 41, and 20 ka BP. Between 113 and 75 ka BP values are generally elevated ranging between ~0.25 and ~0.3% including several low amplitude peaks reaching ~0.35%.

C/N values range between ~3 and ~9 during the last 155 kyr. At orbital scales, C/N show an increasing trend from ~3.5 to ~7.7 between 155 and 111 ka BP, followed by a period of decreasing values between 111 and 67 ka BP. After 67 ka BP, values abruptly increase from 4 to 9, before they progressively decrease again to 3.5 until 25 ka BP. At millennial scales, the temporal variation in C/N is similar to TOC in relation to the occurrence of major peaks.

BGD
8, 2259–2280, 2011

5 Discussion

5.1 Variations of $CaCO_3$, TOC and C/N in relation to global ice volume

Changes in global ice volume are largely represented by benthic $\delta^{18}O$ stacks such as the LR04 benthic stack (Lisiecki and Raymo, 2005) (Fig. 4a). $\delta^{18}O$ maxima between 140 and 135, and 25 and 18 ka BP correspond to the glacial maxima of MIS 6 and MIS 2, respectively, and are associated with distinct increases in TOC and C/N at site PC1, while $CaCO_3$ shows low values during these intervals (Fig. 4). The ice volume advances during MIS 5d and 4 similarly correspond to increased TOC and C/N, and generally decreased $CaCO_3$, although $CaCO_3$ shows a millennial-scale peak during MIS 5d. The abrupt C/N increases at the onset of these two periods occur at times when global ice volume experienced large increases. MIS 5b, on the other hand, is associated with only small amplitude increases of TOC and C/N, but a distinct minimum in $CaCO_3$. Relatively low TOC and C/N, and relatively high $CaCO_3$ correspond to periods of decreased ice volume during MIS 5e, 5c and 5a, but also to the period between 40 and 25 ka BP.

It should be noted that the C/N values in PC1 are generally relatively low, when considering that the Arctic Ocean is dominated by OC_{terr} input, which even today contributes about ~50% of TOC to the Chukchi Borderland region (Naidu et al., 2004; Belicka and Harvey, 2009). We attribute the low C/N values to a generally elevated contribution of N_{inorg} due to low absolute TOC values (<0.5%) (Stein, 2008) at site PC1. In view of the relatively good correlation between TOC and C/N in PC1 we suggest that the relative variations in C and N are controlled by input of organic matter, rather than variation in N_{inorg}. We here therefore interpret changes in C/N as a first-order indicator of relative contributions of OC_{terr} and OC_{mar} to sediment input at site PC1.

BGD

8, 2259–2280, 2011

5.2 Variations of $CaCO_3$, TOC and C/N in relation to northern hemispheric high latitude temperature

$\delta^{18}O$ of the NGRIP ice core (NGRIP members, 2004) (Fig. 4b) reflect the temperature of the high latitude Northern Hemisphere. The millennial-scale abrupt temperature fluctuations during the last glacial period (Dansgaard-Oeschger Cycles, DOC) recorded in NGRIP indicate dramatic climate changes in response to internal climate feedbacks, possibly modulated by variations in solar forcing (Braun et al., 2005). A close comparison of our data with the NGRIP ice core suggests that millennial-scale increases in TOC and C/N can be correlated to Dansgaard-Oeschger Stadials (DOS) 26 to 23 (and/or 22), 21 to 18, as well as DOS 15/16, 13 and 9 (Fig. 4). DOS 18, 13 and 9 correspond to Heinrich events H6, H5 and H4 (e.g. Hemming, 2004). On the basis of this correlation, decreases in $CaCO_3$ correlate to DOS 26 to 23 (and/or 22), 19, 18, 15/16, and 9 (Fig. 4). It should be noted that these correlations are associated with uncertainties due to the nature of our age model, but the good correspondence in timing, amplitude and period length of increases in TOC, C/N and decreases in NGRIP $\delta^{18}O$ supports our suggestion that TOC and C/N increases would have been generally associated with cold stadial episodes of the last glacial period.

5.3 Orbital-scale TOC and C/N variations in response to ice sheet dynamics

The last two glacial-interglacial cycles were characterized by a dynamic waxing and waning of large ice sheets in the Arctic (e.g. Knies et al., 1999, 2000; Müller et al., 1999). For instance, during the global ice sheet advances MIS 6, 4 and 2, voluminous ice sheets covered the land and adjacent shelves of the western Eurasian Arctic, the Canadian Arctic and Greenland (Figs. 1 and 4f). TOC contents in Arctic Ocean sediments in relative proximity to the western Siberian Arctic show distinct increases during these time intervals, which can be well correlated between sediment cores (e.g. Winkelmann et al., 2007, 2008). Primary processes for land-ocean transport of OC_{terr} in the Arctic Ocean are coastal erosion and river discharge (Reimnitz et al., 1988;

BGD
8, 2259–2280, 2011

Rachold et al., 2000; Stein, 2008), importantly supplemented during glacial periods by bedrock-eroded material carried by ice streams and ice sheet flows to the shelf edge (e.g. Elverhøi et al., 1998, Dowdeswell et al., 2002). OC_{terr} is further transported by surface and deep currents, sea ice and icebergs to the open ocean (Stein and Korolev, 1994).

TOC values at site PC1 are generally low, but nonetheless characterized by distinct peaks, in particular during MIS 6, 4 and 2, related to OC_{terr} influx judging from coeval increases in C/N (Fig. 4). We therefore suggest that a fraction of bedrock-derived organic material delivered to the shelf breaks of the Eurasian Arctic due to glacial erosion during MIS 6, 4 and 2 was transported eastward to the Chukchi Borderland as fine suspended matter under the influence of eastward flowing intermediate waters of the Atlantic Layer and/or eastward flowing surface currents and sea ice. Compared to the western Siberian Arctic, dominated by the Barents Sea Ice Sheet, ice sheets of the eastern Siberian Arctic were small or stable with restricted fluctuations during the last glacial period (Knies et al., 2000, 2001; Svendsen et al., 2004). In particular the LGM appears to have been largely free of large ice sheets in Eastern Siberia (e.g. Polyak et al., 2000). Nonetheless, several increases of ice sheets extending to the shelves off eastern Severnaya Zemlya (Knies et al., 1999, 2000) and East Siberia (Müller, 1999) during MIS 6, 5d, 4 and to a lesser extent MIS 5b and 3 (Fig. 4f) may have additionally contributed to OC_{terr} input at site PC1 due to their relative proximity to the Chukchi Borderland.

5.4 Anti-correlation of $CaCO_3$ and TOC and their possible relation to oceanic and atmospheric circulation

As stated in Sect. 4.1.1, increases in detrital $CaCO_3$ at site PC1 were probably associated with enhanced advection of carbonate-rich sediments via sediment-laden sea ice and/or icebergs from the Canadian Arctic in association with an extended Beaufort Gyre during warm periods (Phillips and Grantz, 2001). On the other hand, during cold periods that are associated with lower amounts of $CaCO_3$ and increased values of

BGD
8, 2259–2280, 2011

TOC at site PC1, the Beaufort Gyre contracted and the Transpolar Drift shifted towards North America. We thus suggest that OC_{terr} increases observed at site PC1 derived from the Siberian ice sheets due to glacial erosion, at times when sediment input from the Canadian Arctic decreased due to a weaker Beaufort Gyre. The anti-correlation of $CaCO_3$ and TOC (as well as C/N) at site PC1 may therefore be related to a glacial-interglacial change in major Arctic Ocean current systems (Phillips and Grantz, 2001). Varying IRD input in PC1 provides some additional evidence to such inference (Fig. 4g): increased levels of IRD during MIS 5e, 5a and MIS 3 may be related to sea ice and/or iceberg advection by the Beaufort Gyre. In contrast, rather low IRD occurrences during periods of large Eurasian ice sheets (Fig. 4f and g) could be related to a weaker Beaufort Gyre and calm conditions with sea ice coverage over most of the year. The resultant decrease in marine productivity could have contributed to C/N increases during those intervals. Today, changes in Beaufort Gyre strength are coupled to the Arctic Oscillation (AO) (Thompson and Wallace, 1998): A negative AO is associated with an extended Beaufort Gyre, while a positive AO is associated with a contracted Beaufort Gyre and an extended cyclonic circulation over the Arctic Basin (Mysak, 2001; Rigor et al., 2002; Darby and Bischof, 2004).

5.5 Millennial-scale TOC, C/N and $CaCO_3$ variability in response to DOC and Bering Strait flow

TOC and $CaCO_3$ accumulation at site PC1 did not only respond to slow orbital-scale changes in global ice volume, but also to abrupt millennial-scale variations in northern hemispheric temperature recorded in the NGRIP ice core, based on a good correlation of almost all DOS events between 120 and 40 ka BP with increases in TOC and C/N and in many cases with decreases in $CaCO_3$. Because atmospheric circulation responds immediately to hemispheric temperature changes, we suggest that one possible explanation for these millennial-scale variations in TOC and $CaCO_3$ are changes in AO and consequent changes in the Beaufort Gyre strength. In analogy to orbital-scale variations in Beaufort Gyre strength, discussed in Sect. 5.4, a negative AO during

BGD
8, 2259–2280, 2011

interstadials would have generally led to a Beaufort Gyre extension decreasing OC_{terr} advection from the Siberian shelves and increasing $CaCO_3$ from the Canadian Arctic, while a positive AO during stadials would have led to a Beaufort Gyre contraction associated with increasing OC_{terr} and lower $CaCO_3$.

During MIS 4 and the earlier part of MIS 3 (~65 to ~40 ka BP) TOC and C/N seem to have responded in a particularly sensitive manner to DOC, as they show considerable relative increases during periods that we suggest to correlate to DOS 19, H6, DOS 15/16, H5 and H4. We suggest that TOC events at site PC1 were amplified during those periods in response to millennial-scale shallowing or closures of the Bering Strait during cold stadials of MIS 4 and 3 (Hu et al., 2010), significantly decreasing sea surface temperature and primary productivity in the Chukchi Sea and Chukchi Borderland due to inhibition of nutrient-rich Pacific water influx. A very shallow or closed Bering Strait may have increased coastal erosion along the new continuous coast line and inhibited dilution of Arctic water masses by Pacific waters. Both processes could have led to relative increases of TOC. Our results suggest that the far western Arctic and Chukchi Sea areas were climatically not stable during the last glacial period, but experienced significant and abrupt changes in accordance with northern hemispheric climate change and Bering Strait dynamics.

6 Summary and conclusion

In the present study we discussed orbital- and millennial-scale variations in TOC, C/N and $CaCO_3$ in the Chukchi Borderland in association with glacial-interglacial changes in ice volume and northern hemispheric temperature. Based on a preliminary but substantiated age model, we suggested that orbital- and millennial-scale increases of OC_{terr} in PC1 were related to glacial erosion during cold episodes of the last two glacial-interglacial cycles and decreased marine productivity, while periods of increased $CaCO_3$ were related to advection of carbonate-rich sediments from the Canadian Arctic and increased marine productivity during warm episodes. We propose that

BGD

8, 2259–2280, 2011

Sedimentary organic matter variations in the Chukchi Borderland

S. F. Rella and M. Uchida

this pattern, in particular in view of a good correlation between TOC events and DOS, could be explained by changes in dominant atmospheric surface pressure patterns expressed in mode shifts of the AO. A dominantly positive AO during glacial and stadial periods would have promoted a contracted Beaufort Gyre and an extended cyclonic circulation in the Arctic Ocean facilitating advection of OC_{terr} by the eastward flowing Atlantic Layer and/or eastward flowing surface currents and sea ice to the Northwind Ridge. A prevailing negative AO during warm episodes, on the other hand, would have promoted an extended and strengthened Beaufort Gyre associated with enhanced advection of detrital $CaCO_3$ by sea ice and icebergs to the Northwind Ridge. Observed TOC, C/N and $CaCO_3$ fluctuations in this study suggest that the Arctic responded sensitively to climate changes of the last two glacial-interglacial cycles on both orbital and millennial time scales through changes in marine productivity as well as oceanic and atmospheric circulation patterns, which supports scenarios of an amplified Arctic environmental change in response to modern climate change.

Acknowledgements. We thank M. Utsumi, C. Sato and Y. Kuroki for sampling the cores together with MU during cruise MR08-04 of R/V Mirai. We also thank the captain and crew of the cruise, the staff of Marine Works Japan and the scientific party for their cooperation at sea. We are grateful to M. Kondo, A. Matsuda and T. Tsubata for sample preparation prior to CHN measurements. This study was partly supported by KAKENHI-KIBAN-B (No. 121061 and No. 121552).

References

Backman, J., Jakobsson, M., Løvlie, R., Polyak, L., and Febo, L. A.: Is the central Arctic Ocean a sediment starved basin?, Quaternary Sci. Rev., 23, 1435–1454, 2004.

Belicka, L. L. and Harvey, H. R.: The sequestration of terrestrial organic carbon in Arctic Ocean sediments: a comparison and methods and implications for regional carbon budgets, Geochim. Cosmochim. Ac., 73, 6231–6248, 2009.

Bischof, J. F. and Darby, D. A.: Mid to Late Pleistocene ice drift in the western Arctic Ocean: evidence for a different circulation in the past, Science, 277, 74–78, 1997.

Bordowskiy, O. K.: Sources of organic matter in marine basins, Mar. Geol., 3, 5–31, 1965a.
Bordowskiy, O. K.: Accumulation of organic matter in bottom sediments, Mar. Geol., 3, 33–82, 1965b.
Braun, H., Christl, M., Rahmstorf, S., Ganopolski, A., Mangini, A., Kubatzki, C., Roth, K., and Kromer, B.: Solar forcing of abrupt glacial climate change in a coupled climate system model, Nature, 438, 208–211, 2005.
Darby, D. A. and Bischof, J. F.: A Holocene record of changing Arctic Ocean ice drift, analogous to the effects of the Arctic Oscillation, Paleoceanography, 19, PA1027, doi:10.1029/2003PA000961, 2004.
Darby, D. A., Bischof, J. F., and Jones, G. A.: Radiocarbon chronology of depositional regimes in the western Arctic Ocean, Deep-Sea Res. Pt. II, 44(8), 1745–1757, 1997.
Dowdeswell, J. A., Elverhøi, A., and Spielhagen, R.: Glaciomarine sedimentary processes and facies on the Polar North Atlantic margins, Quaternary Sci. Rev., 17, 243–272, 1998.
Dowdeswell, J. A., Cofaigh, C., Ó, Taylor, J., Kenyon, N. H., Mienert, J., and Wilken, M.: On the architecture of high-latitude continental margins: The influence of ice-sheet and sea-ice processes in the Polar North Atlantic, in: Glacier influenced sedimentation on high-latitude continental margins, edited by: Dowdeswell, J. A. and Cofaigh, C. Ó, Geological Society of London (Special Publication), 203, 33–54, 2002.
Elverhøi, A., Dowdeswell, J. A., Funder, S., Mangerud, J., and Stein, R. (Eds.): Glacial and oceanic history of the Polar North Atlantic margins, Quaternary Sci. Rev., 17, 1–10, 1998.
Hemming, S. R.: Heinrich events: Massive late Pleistocene detritus layers of the North Atlantic and their global climate imprint, Rev. Geophys., 42, RG1005, doi:10.1029/2003RG000128, 2004.
Hu, A., Meehl, G. A., Otto-Bliesner, B. L., Waelbroeck, C., Han, W., Loutre, M.-F., Lambeck, K., Mitrovica, J. X., and Rosenbloom, N.: Influence of Bering Strait flow and North Atlantic circulation on glacial sea-level changes, Nat. Geosci., 729(3), 118–121, 2010.
Johannessen, O. M., Bengtsson, L., Miles, M. W., Kuymina, S. I., Semenov, V. A., Alekseev, G. V., Nagurnyi, A. P., Yakharov, V. F., Bobylev, L. P., Petterson, L. H., Hasselmann, K., and Cattle, H. P., Arctic climate change, observed and modelled temperature and sea-ice variability, Tellus, 56A(4), 328–341, 2004.
Josenhans, H. W., Zevenhuizen, J., and Klassen, R. A.: The Quaternary geology of the Labrador Shelf, Can. J. Earth Sci., 23, 1190–1213, 1986.
Knies, J., Vogt, C., and Stein, R.: Late quaternary growth and decay of the Svalbard-Barents-

BGD
8, 2259–2280, 2011

Sedimentary organic matter variations in the Chukchi Borderland

S. F. Rella and M. Uchida

Sea ice sheet and paleoceanographic evolution in the adjacent Arctic Ocean, Geo-Mar. Lett., 18, 195–202, 1999.
Knies, J., Müller, C., Nowaczyk, N., Vogt, C., and Stein, R.: A multiproxy approach to reconstruct the environmental changes along the Eurasian continental margin over the last 150000 years, Mar. Geol., 163, 317–344, 2000.
Knies, J., Kleiber, H. P., Matthiessen, J., Müller, C., and Nowaczyk, N.: Marine ice-rafted debris records constrain maximum extent of Saalian and Weichselian ice-sheets along the northern Eurasian margin, Global Planet. Change, 31, 45–64, 2001.
Lisiecki, L. E. and Raymo, M. E.: A Pliocene-Pleistocene stack of 57 globally distributed benthic δ18O records, Paleoceanography, 20, PA1003, doi:10.1029/2004PA001071, 2005.
Macdonald, R. W., Solomon, S. M., Cranston, R. E., Welch, H. E., Yunker. M. B., and Gobeil, C.: A sediment and organic carbon budget for the Canadian Beaufort Shelf, Mar. Geol., 144, 255–273, 1998.
Macdonald, R. W., Harner, T., Fyfe, J., Loeng, H., and Weingartner, T.: AMAP Assessment 2002: The influence of global change on contaminant pathways to, within, and from the Arctic, Arctic Monitoring and Assessment Programme (AMAP), Scientific Report, Oslo, 65 pp., 2003
Müller, C.: Rekonstruktion der Paläo-Umweltbedingungen am Laptev-See-Kontinentalrand während der beiden letzten Glazial-/Interglazial-Zyklen anhand sedimentologischer und mineralogischer Untersuchungen, Report on Polar Research, 328, 146 pp., 1999.
Mysak, L. A.: Patterns of Arctic circulation, Science, 293, 1269–1270, 2001.
Naidu, A. S., Cooper, L. W., Grebmeier, J. M., Whitledge, T. E., and Hameedi, M. J.: The continental margin of the North Bering-Chukchi Sea: Distribution, sources, fluxes, and burial rates of organic carbon, in: The organic carbon cycle in the Arctic Ocean, edited by: Stein, R. and Macdonald , R. W., Heidelberg, Springer-Verlag, 193–203, 2004.
NGRIP members: High-resolution record of Northern Hemisphere climate extending into the last interglacial period, Nature, 431, 147–151, 2004.
Phillips, R. L. and Grantz, A.: Quaternary history of sea ice and paleoclimate in the Amerasia Basin, Arctic Ocean, as recorded in the cyclical strata or Northwind Ridge, Geol. Soc. Am. Bull., 109, 1101–1115, 1997.
Phillips, R. L. and Grantz, A.: Regional variations in provenance and abundance of ice-rafted clasts in Arctic Ocean sediments: Implications for the configuration of Late Quaternary oceanic and atmospheric circulation in the Arctic, Mar. Geol., 172, 91–115, 2001.

BGD
8, 2259–2280, 2011

Polyak, L. V., Gataullin, V., Epshtein, O., Okuneva, O., and Stelle, V.: New constraints on the limits of the Barents-Kara ice sheet during the Last Glacial Maximum based on borehole stratigraphy from the Pechora Sea, Geology, 28, 611–614, 2000.

Rachold, V., Grigoriev, M. N., Are, F. E., Solomon, S., Reimnitz, E., Kassens, H., and Antonow, M.: Coastal erosion vs riverine sediment discharge in the Arctic shelf seas, Int. J. Earth Sci., 89, 450–460, 2000.

Reimnitz, E., Graves, S. M., and Barnes, P. W.: Beaufort Sea coastal erosion, sediment flux, shoreline evolution and the erosional shelf profile, US Geological Survey, 22 pp., 1988.

Rigor, I. G., Wallace, J. M., and Colony, R. L.: On the response of sea ice to the Arctic Oscillation, J. Climate, 15, 2648–2668, 2002.

Shipp, S. S., Wellner, J. S., and Anderson, J. B.: Retreat signature of a polar ice stream: Sub-glacial geomorphic features and sediments from the Ross Sea, Antarctica. In:Glacier influenced sedimentation on high-latitude continental margins, edited by: Dowdeswell, J. A. and Cofaigh, C. Ó., Geological Society of London (Special Publication 203), 277–304, 2002.

Spielhagen, R. F., Bonani, G., Eisenhauer, A., Frank, M., Frederichs, T., Kassens, H., Kubik, P. W., Mangini, A., Nörgaard-Pedersen, N., Nowaczyk, N. R., Schäper, S., Stein, R., Thiede, J., Tiedemann, R., and Wahsner, M.: Arctic Ocean evidence for Late Quaternary initiation of northern Eurasian ice sheets, Geology, 25, 783–786, 1997.

Spielhagen, R. F., Baumann, K.-H., Erlenkeuser, H., Nowaczyk, N. R., Nørgaard-Pedersen, N., Vogt, C., and Weiel, D.: Arctic Ocean deep-sea record of Northern Eurasian ice sheet history, Quaternary Sci. Rev., 23 (11–13), 1455–1483, 2004.

Stein, R.: Arctic Ocean Sediments: Processes, Proxies, and Paleoenvironment, Developments in Marine Geology, Elsevier, Amsterdam, 2, 592, 2008.

Stein, R. and Korolev, S.: Shelf-to-basin sediment transport in the eastern Arctic Ocean, Report on Polar Research, 144, 87–100, 1994.

Svendsen, J. I., Alexanderson, H., Astakhov, V. I., Demidov, I., Dowdeswell, J. A., Funder, S., Gataullin, V., Henriksen, M., Hjort, C., Houmark-Nielsen, M., Hubberten, H. W., Ingolfsson, O., Jakobsson, M., Kjaer, K. H., Larsen, E., Lokrantz, H., Lunkka, J. P., Lysa, A., Mangerud, J., Matiouchkov, A., Murray, A., Moller, P., Niessen, F., Nikolskaya, O., Polyak, L., Saarnisto, M., Siegert, C., Siegert, M. J., Spielhagen, R. F., and Stein, R.: Late quaternary ice sheet history of northern Eurasia, Quaternary Sci. Rev., 23, 1229–1272, 2004.

Thompson, D. W. J. and Wallace, J. M.: The Arctic Oscillation signature in the wintertime geopotential height and temperature fields, Geophys. Res. Lett., 29(9), 1297–1300, 1998.

BGD

8, 2259–2280, 2011

Sedimentary organic matter variations in the Chukchi Borderland

S. F. Rella and M. Uchida

Winkelmann, D.: Sediment dynamics of megaslides along the Svalbard continental margin and the relation to paleoenvironmental changes and climate history, unpublished Ph.D. thesis, Bremen University, 180 pp., 2007.
Winkelmann, D., Schäfer, C., Stein, R. and Mackensen, A.: Terrigenous events and climate history within the Sophia Basin, Arctic Ocean, Geochem. Geophy. Geosy., 9, Q07023, doi:10.1029/2008GC002038, 2008.
Wollenburg, J. E. and Mackensen, A.: Living benthic foraminifers from the central Arctic Ocean: Faunal composition, standing stock and diversity, Mar. Micropaleontol., 34, 153–185, 1998.

BGD
8, 2259–2280, 2011

Sedimentary organic matter variations in the Chukchi Borderland

S. F. Rella and M. Uchida

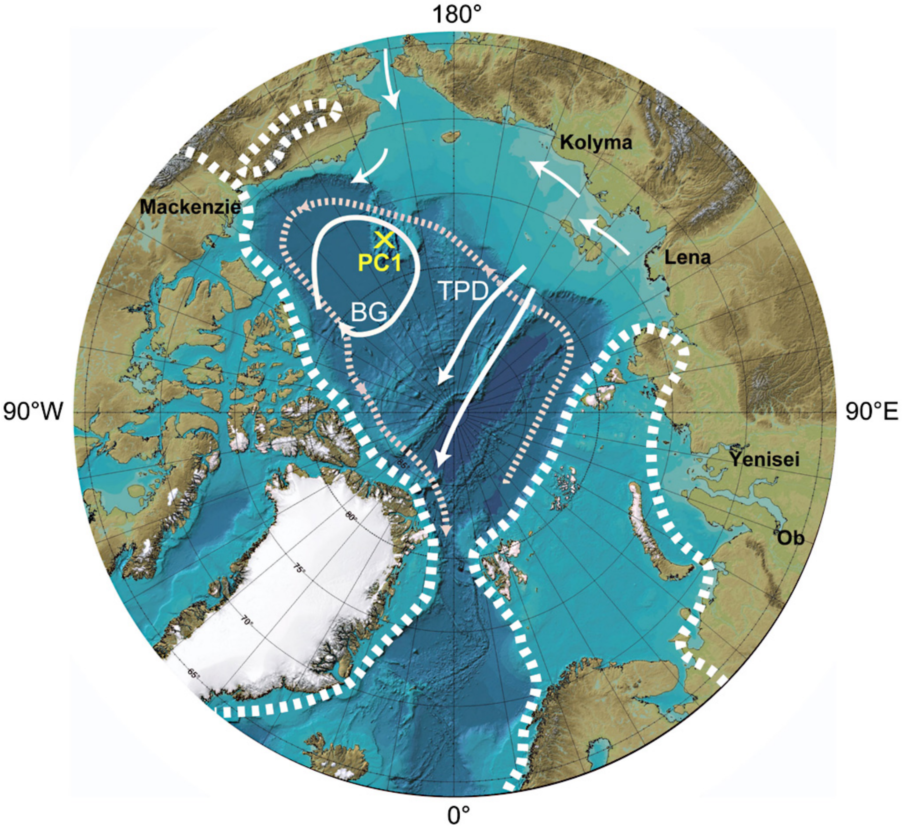

Fig. 1. Map of the Arctic Ocean and adjacent land masses. Location of PC1 is indicated by an "x". Modern surface currents are shown as white arrows (BG = Beaufort Gyre; TPD = Transpolar Drift), and the Atlantic Layer intermediate water flow as dashed grey arrow. The white dashed lines denote extents of reconstructed LGM ice sheets (Svendsen et al., 2004). The names of large rivers are indicated at their present location.

BGD
8, 2259–2280, 2011

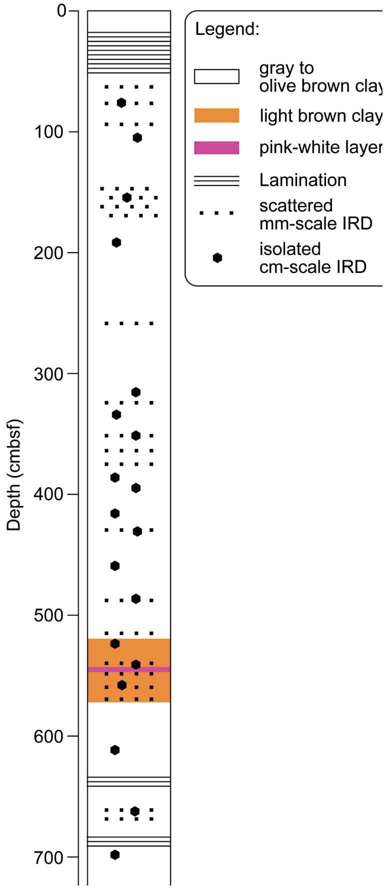

Fig. 2. Columnar section of PC1. Laminated horizons, and horizons with scattered mm-scale and isolated cm-scale IRD based on visual core inspection and soft-X ray radiographs are indicated. The light brown layer between 520 and 572 cmbsf and the pink-white layer between 539 and 543 cmbsf are also shown.

BGD
8, 2259–2280, 2011

Sedimentary organic matter variations in the Chukchi Borderland

S. F. Rella and M. Uchida

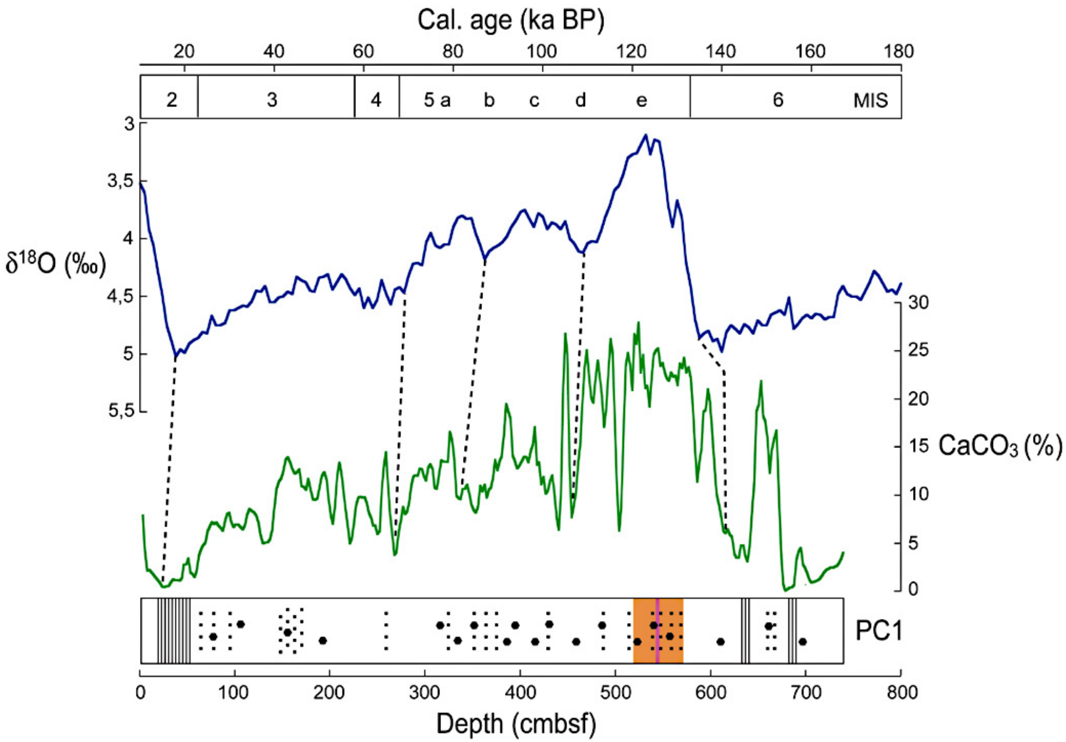

Fig. 3. An age model for PC1. The variation of $CaCO_3$ in PC1 with depth is compared to the LR04 benthic $\delta^{18}O$ stack (Lisiecki and Raymo, 2005). Dashed lines indicate the proposed correlation between the two records. The columnar section of PC1 is also shown (the legend is the same as in Fig. 2). MIS stages are shown on top.

BGD
8, 2259–2280, 2011

Title Page
Abstract Introduction
Conclusions References
Tables Figures
◂I ▸I
◂ ▸
Back Close
Full Screen / Esc
Printer-friendly Version
Interactive Discussion

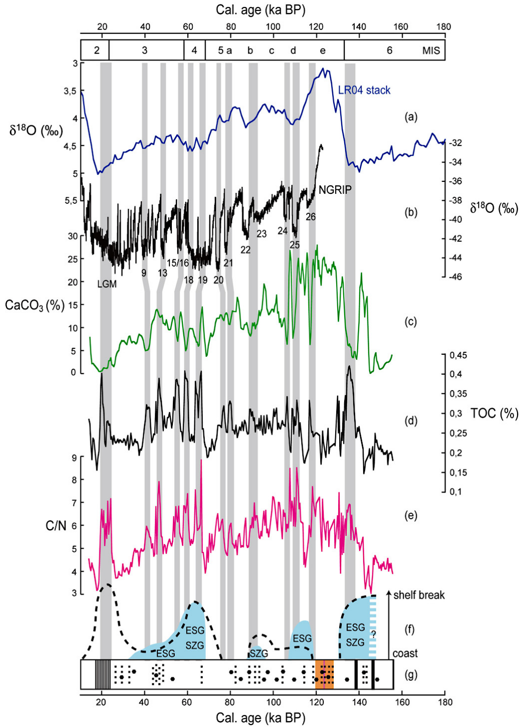

Fig. 4. Temporal variations of **(a)** the LR04 benthic $\delta^{18}O$ stack (Lisiecki and Raymo, 2005), **(b)** the NGRIP $\delta^{18}O$ record (NGRIP members, 2004), **(c)** $CaCO_3$ of PC1, **(d)** TOC of PC1, **(e)** C/N of PC1. Panel **(f)** shows the temporal variations in the extent of Eurasian ice sheets between the coast and the shelf break. Extents of the East Siberian Glaciation (ESG) and the Severnaya Zemlya Glaciation (SZG) are indicated as blue shadings. Extents of the Northern Barents Sea Ice Sheet are indicated as dashed black line. The columnar section of PC1 is shown in panel **(g)** (the legend is the same as in Fig. 2). MIS stages are shown on top. Vertical grey shadings indicate relative increases of TOC and their possible relation to DOS. Corresponding stadial numbers are shown in panel **(b)**.

BGD

8, 2259–2280, 2011